©JoESE
Publisher ISES 2014

http://www.joes.org.in

Journal of Earthquake Science and Engineering, Vol-1, PP 59-79

Multifractal Detrended Fluctuation Analysis of Seismic Induced Radon-222 Time Series

Chiranjib Barman[1,*], Hirok Chaudhuri[1], Debasis Ghose[1], Argha Deb [2], Bikash Sinha[1]

[1]Variable Energy Cyclotron Centre, Department of Atomic Energy, Kolkata, India

[2] Physics Department, Jadavpur University

Received: 06/05/2013; Accepted: 13/03/2014

Abstract

"Multifractal detrended fluctuation analysis (MFDFA)" is a relatively new technique in the domain of nonlinear analysis and widely used to bring out the information hidden in a time series data. The essence of MFDFA lies in overcoming various restrictions or limitations of the "detrended fluctuation analysis (DFA)" technique. In the present paper, we have applied MFDFA technique on soil radon-222 time series with an aim to understand the underlying dynamics of seismic induced soil gas anomaly. Several, multifractal parameters especially the generalized Hurst exponent, scaling exponent as well as the multifractal spectrum of the soil radon-222 time series were figured out. Results show that soil radon-222 time series data consists of several nonlinear features such as fractal structures, long range correlation etc. which may have originated out of a wide range of perturbations generated by seismic induced physico-chemical disturbances within the earth's crust. The estimated local fluctuations or root mean square (RMS) values greatly assist to figure out the anomalous pattern present in the said radon-222 time series. The MFDFA technique seems to be prospective in earthquake precursor study.

Keywords: Multifractal, Hurst exponent, Long range correlation, Soil radon-222, Geochemical precursor, Earthquake prediction

1. Introduction

It is well documented in the literature that the abnormal fluctuation observed in the radon-222 emanations from sub-soil gases as well as hydrothermal gases serve as a geochemical tracer for an imminent seismic event (Cicerone et al., 2009; Hartmann and Levy, 2005; Toutain and Baubron, 1999). The most interesting feature is that secular equilibrium of the radioactive element radon-222 emanating from the earth's interior is greatly influenced by

* Corresponding author:
E-mail address: cbarman@vecc.gov.in (C. Barman)

tectonic activities, namely the changes in physico-chemical processes of the under-earth fluid reservoir and alteration in stress-strain pattern of the earth's crust during the final stage of earthquake preparation phase just before rupture (Planinic et al., 2004; Wakita, 1996; Hauksson and Goddard, 1981; King, 1980). However, the diffusion and advection mechanism for soil radon emanation process are also controlled by several geophysical and geochemical factors such as (i) geomorphology of the study area, (ii) existence of geological fault in the vicinity of the study area, (iii) soil porosity, (iv) ground water movement, (v) distribution of uranium and radium in the bed rock, (vi) micro seismicity in the region etc. (Chaudhuri et al., 2012, 2010a; Ramola et al., 2008; Das et al., 2006a; Walia et al., 2003; Abumuard and Al-Tamimi, 2001;Ball, 1994; Virk and Singh, 1993; Igarashi and Wakita, 1990; Nazaroff and Nero, 1988; Holub and Brady, 1981; Schynoll and Chatterjee, 1958). The earth's tide (periodic or semiperiodic), meteorological parameters such as ambient humidity, ambient temperature, ambient pressure, rainfall and soil characteristics such as soil moisture, soil temperature, soil pressure, soil porosity etc. also play vital role in the radon emanation process from sub-soil gases (Chaudhuri et al, 2011, 2010b; Weinlich et al., 2006; Prasad et al., 2006, Barnet et al., 1997). The entire soil radon emanation process is a complex phenomena. To understand the dynamics of radon emanation process and its relation with tectonic activities several attempts have been made world wide since the last three decades (Chaudhuri et al., 2013a; 2013b; Cicerone et al., 2009; Ghosh et al., 2009; Toutain and Baubron, 1999). Various mathematical modelings were also proposed by some workers (Omar et al., 2013; Fleischer R L, 1981; Walia et al., 2005; Kumar et al., 2012; Walia et al., 2005a). However, as per our present understanding it is very difficult to explore the complex phenomena of seismic induced radon emanation process by means of conventional mathematical modeling and statistical analysis. Nonlinear methods such as power spectrum analysis, wavelet analysis, fractal analysis etc. may assist to reveal nonlinear characteristics of the underearth physico-chemical mechanism involved in radon emanation process (Chaudhuri et al., 2013a; 2013b; Das et al., 2006b).

With an aim to explore the dynamics of soil radon emanation process and its relation with seismicity in the present paper we have performed "multifractal detrended fluctuation analysis (MFDFA)" of the soil radon-222 time series data. In this section we have briefly described the principles of MFDFA. The technique MFDFA is a modified and more generalised form of the well known fractal analysis which is frequently used to understand different complex phenomena related with space-physics (Hu J et al., 2009; Movahed M S et al., 2006), bio-physics (Ihlen, 2012; Peng et al., 1994), medical science (Dutta, 2010a; Ivanov et al., 1999; Stanley 1999), material science (Kantelhardt et al., 1999; Vandewalle et al., 1999), weather forcasting (Deidda, 2000; Tessier et al., 1993), stock market (Dutta, 2010b; Liu et al., 1999) and even in earth sciences (Ghosh et al., 2012; Telesca et al., 2006, 2005; Ashkenazy et al., 2003a, 2003b). The fractal analysis demonstrates the characteristics of the natural systems that exhibit irregular pattern at all scales i.e. every

phase of the system. In general 'fractals' are classified into two categories: (i) monofractals and (ii) multifractals. In monofractals the scaling properties of the system remain same in different phases of the system viz. one single scaling exponent is sufficient to describe the scaling properties of the sytem. On the other hand 'multifractals' are more complicated self-similar processes that consist of a number of weighted fractals with different non-integer dimensions. In case of multifractals the scaling properties are dissimilar in diffferent phases (segments) of the system both in time domain as well as in frequency domain. Consequently, multifractal systems require at least more than one scaling exponent to describe the scaling properties of the sytem (Chen et al., 2002). It is to be noted that any natural system does not exhibit simple monofractal behaviour (Chen et al., 2002; Kantelhardt et al., 2001; Hu et al., 2001). Therefore, it is absolutely essential to apply multifractal analysis to the time series data related with a natural process to understand the underlying physics of the complex system. In the present work, we have applied the technique of MFDFA to the soil radon time series data recorded at Tattapani geochemical monitoring laboratory, Jammu & Kashmir (J & K), India during the 2 months period (November 5-December 31, 2012). During this period the ambient temperature remains relatively dry and stable, so that the disparity between the diurnal average maximum (16^0C) and minimum (9^0C) temperature was the least in comparison to the same at other seasons namely in summer. Additionaly, the influence of rainfall during the mentioned period was less with respect to the same in monsoon.

2. Geological Background of the Study Area- Tattapani hot Spring Site

Soil radon-222 monitoring facility for earthquake precursory study was installed at Tattapani hot spring site (33.24^0N, 74.41^0E) during the mid of August 2012. The springs are situated in proximity to the Main Boundary Thrust (MBT) of the Lesser Himalayas at an altitude of about 800m above mean sea level (Wadia, 1928; Gokam et al., 2002). At Tattapani there are two inferred geothermal channels (Rai et al., 1996). These channels originate out of tear fault created by thrust contact of (a) layered structure of Precambrian age Sirban Limestone succession composed of lamina-scale organic-rich source rocks that unconformably overly (b) calcareous and argillaceous sediments of Subathu Formation of Eocene age (Bhat et al. 2009, Siva, 2011). The rocks of the region have varying ages ranging from Precambrian to recent. The area lies in a high risk zone - "seismic zone IV" as per the seismic zoning map of India. There are two thermal springs at Tattapani with temperatures 55^0C and 46^0C. The thermal springs fall in the vicinity of geologically conjectured faults and contact zones of the mountain formations (Shankar R, 1991; Hassan and Baig, 2006). These faults are east-west facing. The geological settings of the study area are displayed in Fig. 1. Terrestrial gases issuing out of the hot spring at Tattapani are enriched in radon-222 (890 kBq/m^3), helium (1.1 vol.%) and carbon di-oxide (4.9 vol.%) (Chaudhuri et al., 2011).

3. Method of Analysis

We have adopted the method of MFDFA as described by Kantelhardt et al. (2002) to analyze the soil radon time series data. If we consider a time series x(i), where i= 1, 2, …, N, and N is length of the time series, the average value x_{ave} of the time series is estimated by the following mathematical relation

$$x_{ave} = \frac{1}{N}\sum_{k=1}^{N} x(k), \quad (1)$$

where x (k) is the value of x(i) for i=k and k may vary from 1 to N.

Considering x(i) as the increment of a random walk process around the average value x_{ave}, the 'trajectory '(or 'profile') y(i) of the time series is derived by the following relation

$$y(i) = \sum_{k=1}^{i}[x(k) - x_{ave}] \quad (2)$$

The method of integration which is adopted to figure out the trajectory assists to reduce the noise content of the dataset. Subsequently, the integrated time series is divided into N_s number of non-overlapping segments (designated asv) of equal length s. The number of segment N_s is defined by the relation

$$N_s = int\left(N/s\right), \quad (3)$$

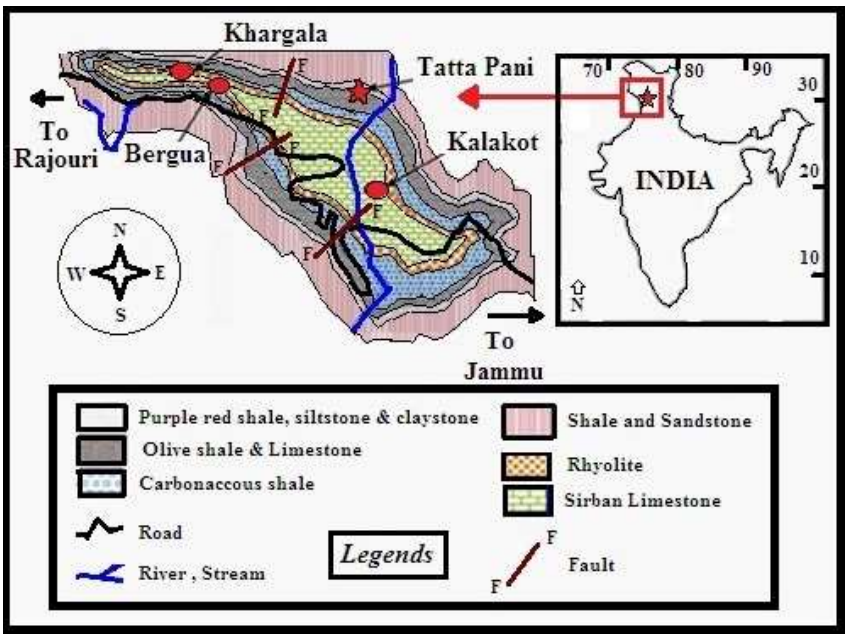

Figure 1. The geological settings of Tattapani geothermal area, J & K.

It is not essential that the length N of the time series always should be an integer multiple of the timescale (s), therefore a short part of the trajectory y(i) may exist at the end of the trajectory. With a view to acquire a high degree of accuracy in estimation process the same procedure (forward direction procedure) is repeated from the opposite end (backward direction procedure) as well. Thereby, $2N_s$ segments are obtained altogether.

The local trend for each of the $2N_s$ segments is now calculated by a least-square fit of the time series. Thereafter, the variance $F^2(s,v)_f$ (forward direction procedure) of each segment v is estimated by

$$F^2(s,v)_f = \frac{1}{s}\sum_{i=1}^{s}[y((v-1)s+i) - y_v(i)]^2 \quad (4)$$

where v may vary from 1 to N_s and y_v is the least-sqare fit of segment v for profile y(i).

Similarly the variance $F^2(s,v)_b$ (backward direction procedure) of each segment v is estimated by

$$F^2(s,v)_b = \frac{1}{s}\sum_{i=1}^{s}[y\{N-(v-N_s)s+i\} - y_v(i)]^2, \quad (5)$$

where v may vary from N_s+1 to $2N_s$.

After detrending the time series, an average is performed over all the segments (v = 1 to 2Ns) to obtain the q^{th} order fluctuation function

$$F_q(s) = [\frac{1}{2N_s}\sum_{v=1}^{2N_s}\{F^2(s,v)^{\frac{q}{2}}\}]^2, \quad (6)$$

where, in general, the index variable q may take any real number other than zero.

Similar procedure is now performed for different values of the time scale length (designated as s) of the segment v. The length 's' theoretically may take any integer value. Now, if the time series x_i is governed by long-range power law correlation, $F_q(s)$ will also follows a power law for large values of s as described below

$$F_q(s) \propto s^{H(q)} \quad (7)$$

The graphical plot of log $F_q(s)$ vs log (s) gives a straight line with slope H(q) for a particular value of q. The log $F_q(s)$ vs log (s) plot should be figured out for different values of q. Now estimating the slope H(q) for each and every value of q, one can determine the scaling behaviour of the fluctuation function $F_q(s)$. 'H(q)' is known as 'generalised Hurst exponent' and varies with q. For a stationary time series second order (for q=2) generalised Hurst exponent ($H_{q=2}$) is identical with the well defined 'Hurst exponent' (Feder, 1988). For the

positive values of q, H_q describes the scaling behaviour of the segments with large fluctuations while the scaling behaviour of the segments with small fluctuations are expressed by H_q for the negative values of q. On the other hand the value of $H_{q=0}$ for q=0 is determined by $\lim_{q \to 0} H_q$. However, the direct averaging procedure as described in equation (6) completely fails to estimate fluctuation function $F_q(s)$ for q=0 due to the diverging nature of the exponent. Thus, a logarithmic averaging procedure is applied to estimate the fluctuation function $F_q(s)$for q=0 (i.e. $F_0(s)$) by means of the following relation,

$$F_0(s) \equiv \exp\left[\frac{1}{4N_s}\sum_{v=1}^{2N_s} \ln(F^2(s,v))\right] \approx s^{H(0)} \quad (8)$$

Now, in order to quantify the multifractality in a time series, the multifractal spectrum D_q is derived by mathematical relation between H_q and classical scaling exponent $\tau(q)$ as described below,

$$\tau(q) = qH(q) - 1, \quad (9)$$

Legendre transform of $\tau(q)$ (Barabási et al. 1991; Feder, 1988) provides the value of Hölder exponent (or singularity strength) h_q as follows ,

$$h_q = \frac{d\tau}{dq} \quad (10)$$

and subsequently the multifractal spectrum D_q which specifies the dimension of subset series (characterised by h_q) is determined by the relation

$$D_q = qh_q - \tau(q) \quad (11)$$

The nature of multifractality of the soil radon-222 time series was also investigated by means of randomly shuffled data set generated out of the original soil radon time series data by the technique followed by Kantelhardt et al. (2002). In principle, the multifractality of a time series may originate (a) either due to presence of broad probability-density function (non Gaussian distribution) of the time series and / or (b) simultaneous existence of dissimilar characteristics of long-range correlations for small as well as large fluctuations or occasionally from (c) combination of both. In order to identify the source we analyzed the randomly shuffled time series of soil radon data. Generally, in the randomly shuffled time series all possible correlations are wiped out by putting the data points into a random fashion. However the probability density function remains unchanged. If the multifractality of the time series is sourced from type (b) the shuffled series will show random behavior with $H_{q,shuf} = 0.5$. On the other hand if the multifractality of the time series is sourced from type (a) the generalised Hurst exponents estimated from original and

shuffled time series will be identical (i.e. $H_{q,original} = H_{q,shuf}$). This happens only because the multifractality depends upon the probability density. Moreover, if the multifractality is sourced from both type (a) and type (b) the shuffled series will exhibit weaker multifractality in comparison to the original time series. The values of classical scaling exponent $\tau(q)$, known as mass exponent (or Rényi exponent), were also estimated for the soil radon time series by means of equation (9) to determine the confinement of nonlinearity. Further, the mutifractal spectrum for the soil radon time series was figured out using the equation (11). The multifractal spectrum gives the detailed quantification of long range correlation characteristics of a time series (Ashkenazy et al., 2003a, 2003b; Shimizu et al., 2002). In particular, the width of a multifractal spectrum is a measure of degree of multifractality present in the time series –"wider the spectrum richer the multifractality" (Telesca et al., 2004). However, for the monofractal data set the width of the spectrum happens to be zero. The particular value of Hölder exponent (i.e. $h_{q,max}$) for which the spectrum reaches its maximum value (i.e. $D_{q,\ max}$) indicates the degree of correlation present in the sample. As the estimated value of $h_{q,max}$ gets lowered the time series shows higher degree of correlation.

Apart from MFDFA of soil radon time series recorded at Tattapani observatory, an attempt was also made to correlate the anomaly observed in the radon time series with subsequent earthquakes that occurred in the region of interest. A number of empirical algorithms, given in the literature, facilitate to identify the patterns of precursory signals that characteristically occur prior to earthquakes (Chaudhuri et al., 2011; Cicerone et al., 2009; Walia et al., 2005b; Talwani., 1979). The empirical algorithms were proposed on the basis of statistical comparison of precursory data with seismic ones, from an existing data base recorded by means of geochemical, hydrological, seismological and electromagnetic techniques related with earthquake precursory studies. The preparation area (or the zone of influence) of an earthquake scales directly with the magnitude M. Maximum limit of the zone of influence (R_{max}) is essentially a geodesic distance (in km) that includes the epicenter of the earthquake and the monitoring stations where significant anomalies can be expected due to seismic activity (Chaudhuri et al., 2013a; 2013b; Walia et al., 2013; Walia et al., 2009). Out of the various empirical relations that connect M to *R*, the equation put forward by

$$R_{max,Fls} = 10^{0.43M} \quad \text{for } M \geq 3 \tag{12}$$

Fleischer (1981) confers the largest value (R_{max}) to the radius of influence (R).

4. Experimental Methodology

In order to monitor radon precursor for imminent seismic events we have set up monitoring facility to continuously record radon-222 concentration in sub-soil gases of

Tattapani geothermal area (Fig.1). Concentration of soil radon-222 (in Bq/m^3) along with soil pressure (in mbar) and soil temperature (in ^0C) are continuously registered by BARASOL BMC2 probe (Algade, France make). All the probes are integrated in a cylindrical chamber was installed at a depth of 2 meter.

The instrumental setup also consists of a pluviometer installed at the earth's surface to acquire the rainfall data of the region. The data registered by different probes are stored in a memory chip which is controlled by a micro-processor embedded in the system. Processing of the recorded data in tabulated form are performed automatically by a software RnView2 and subsequently are transferred to the interfacing server computer. A schematic diagram of the experimental set up is shown in Fig. 2. The data recorded at field laboratory are regularly (daily) transferred to our headquarter at Kolkata by VSAT internet facility to prepare a data bank. Further analysis of data by means of nonlinear analysis is performed at VECC, Kolkata.

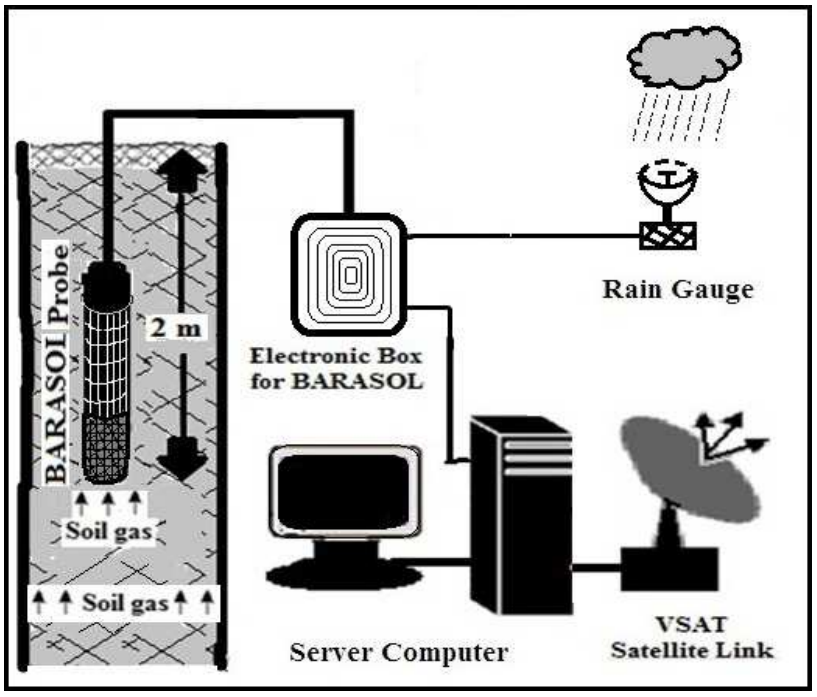

Figure 2. Schematic diagram of the experimental set up for continuous soil radon monitoring.

5. Results and Discussions

Temporal variation of the soil radon data recorded at Tattapani laboratory during the period November 5-December 31, 2012 is shown in Fig. 3 (Panel A). Temporal variation of

soil radon recorded by Barasol probe, estimated values of cubic line interpolation, mean value, mean+2σ (σ is the standard deviation of the data set) and mean-2σ of the soil radon data set are represented by black, red, blue, green and brown symbols respectively in Fig. 3 (panel A). The observed soil radon concentration varied from 2.34 kBq/m^3 to 58.99 kBq/m^3 with an average value 35.50kBq/m^3 and standard deviation 6.75. Four prominent fluctuations (>mean+2σ and also < mean-2σ) are seen in the entire two months radon time series data. Estimation shows that these fluctuations are observed through wide band of data points such as band 1 (data points 52-359), band 2 (data points 2230-2623), band 3 (data points 6673-6730) and band 4 (data points 7754-7859). In data band 1 (i.e. in time frame November 5-7, 2012), data band 2 (i.e. in time frame November 20-23, 2012), data band 3 (i.e. in time frame December 20, 2012) and data band 4 (i.e. in time frame December 28-29, 2012) soil radon concentrations show local minima with value 15.74 kBq/m^3, local maxima with value 58.99 kBq/m^3, local minima with value 12.23 kBq/m^3 and local minima with value 2.34 kBq/m^3 respectively. Variations of soil temperature, soil pressure and rainfall recorded during the mentioned time period are also shown in panel B, panel C and panel D of Fig. 3 respectively. The registered soil temperature at 2 m depth varied from 18.2^{0}C to 25.6^{0}C while sub-soil pressure fluctuated between 914 mbar and 929 mabr. There was no noticeable rainfall during the monitoring period of November 5–December 31, 2012, other than that which was registered by the rain gauge on December 28, 2012. On this day a 1.6 mm rain occurred across a 20 hours duration as shown in Fig.3 (panel D). Any cross-correlation between the temporal variation of concentration profile of soil radon, soil temperature as well as soil pressure was not found. However, interestingly in the region of band 4 (7754-7859) (i.e. in the time frame December 28-29, 2012) the temporal variation in the concentration of soil radon reflects a good anti-coorelation with the rainfall data.

Local fluctuations or root mean square (RMS) plots of the soil radon data are shown in panel A and panel B of Fig. 4 for scale length S=16 and 32 respectively. The method of RMS analysis greatly assist to filter out very small fluctuations (noise) present in the soil radon time series. Moreover RMS technique helps to identfy the genuine fluctuations (large amplitude fluctuations) embedded in the soil radon time series.

Two large amplitude fluctuations are identified in the RMS plot in the data band A (6196-6320) and band B (7262-7440) of Fig. 4. Consequently out of four prominent fluctuations as reflected in Fig. 3 (panel A) only two fluctuations can be statistically valid large amplitude fluctuations (as shown in the Fig. 4). These large amplitude fluctuations correspond to the negative anomalies observed in the soil radon time series data (Fig. 3, panel A) recorded during December 20, 2013 (band 3) and December 28-29, 2013(band 4) respectively. The graphical plot of log Fq(s) vs log (s) for different values of q (q= ±5, 0) is shown in Fig. 5.

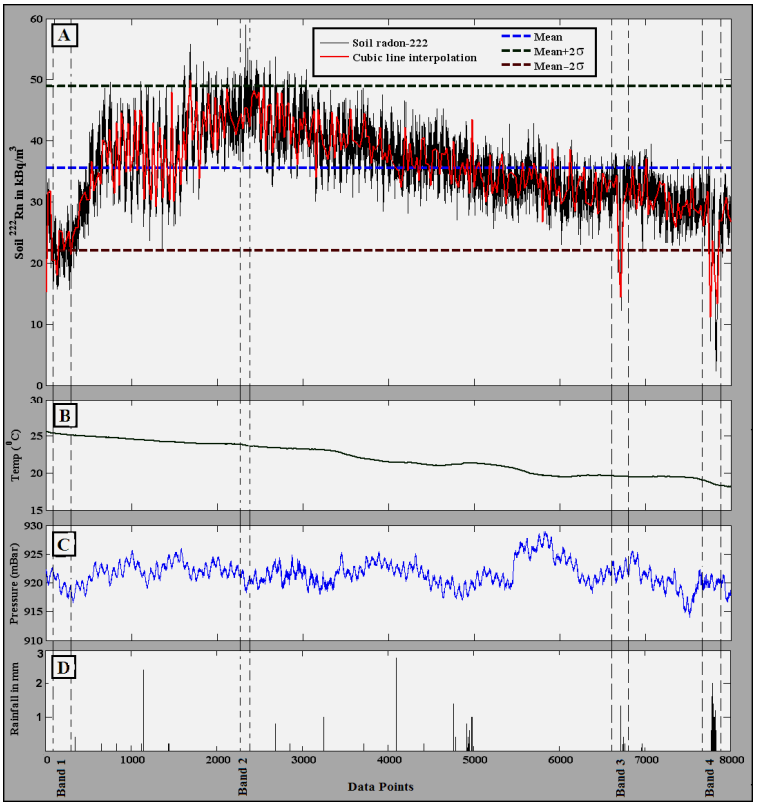

Figure 3. **(A) Temporal variation of soil radon-222 (B) Temporal variation of soil temperature, (C) Temporal variation of soil pressure, (D) Temporal variation of rainfall recorded at Tattapani during the period November 5-December 31, 2012.**

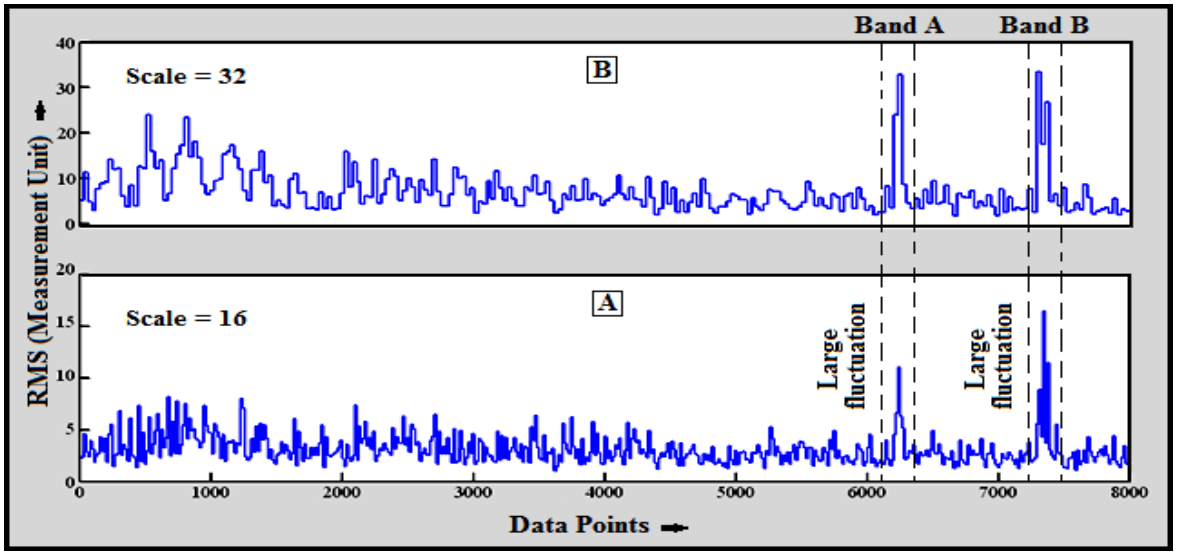

Figure 4. **Variation of RMS (local fluctuation) for the soil radon time series for scale-16 (panel A) and scale-32 (panel B).**

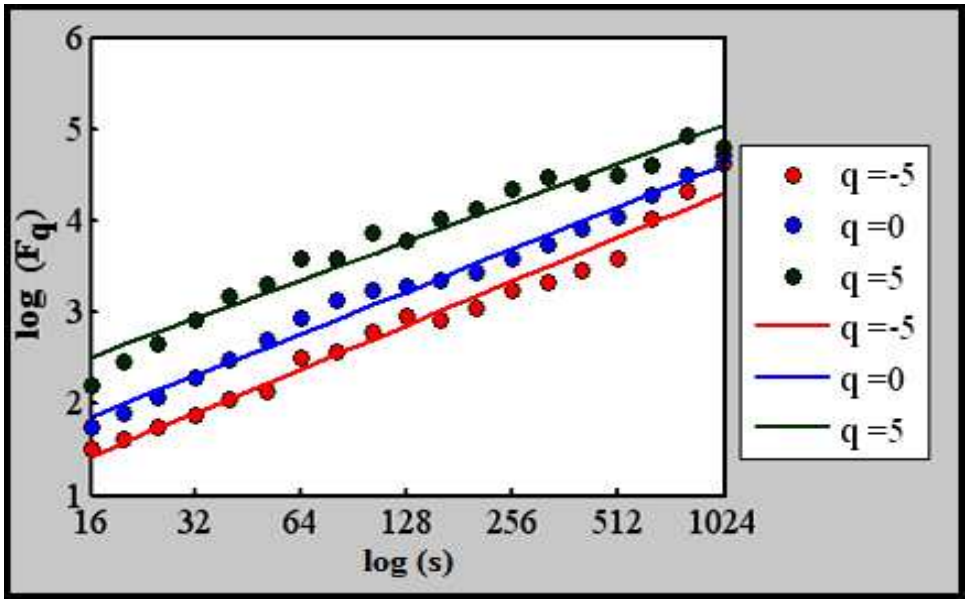

Figure 5. **Log (F_q) vs log (s) plot for q= ±5, 0.**

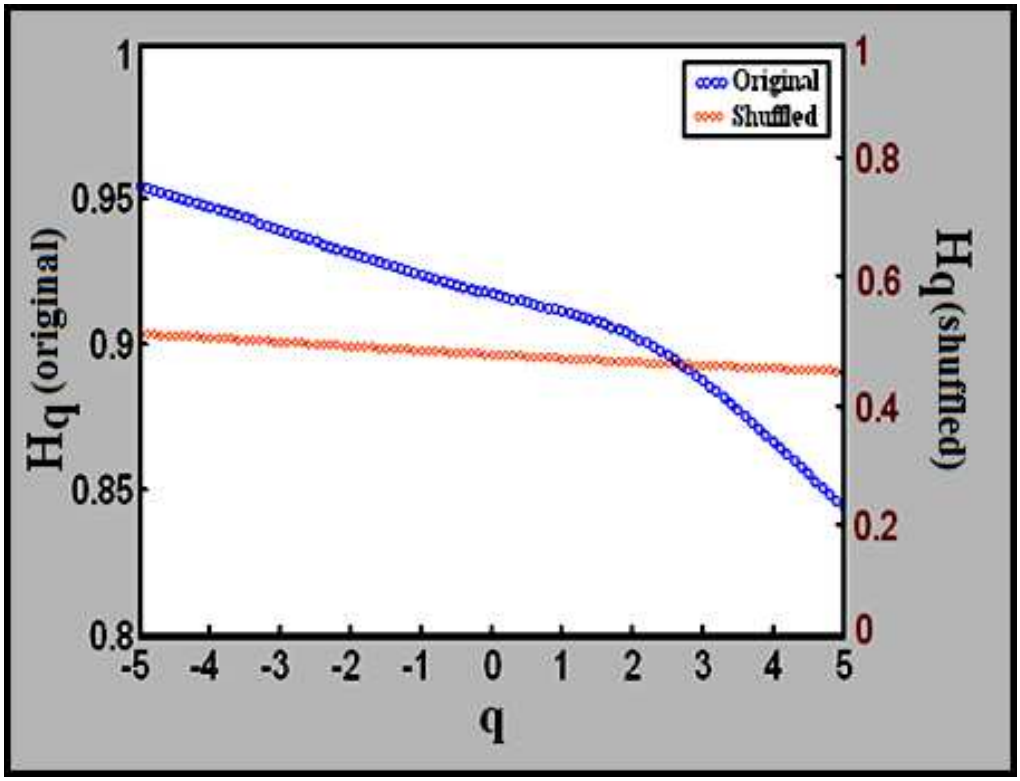

Figure 6. Variation of q^{th} order Hurst exponent (H_q) with q for original time series (blue) and shuffled time series (red).

Variations of log Fq(s) vs log(s) for q=+5, q=0 and q= -5 are marked as green, blue and red symbols respectively. The dots represent the values of the log Fq(s) for different values of log (s) where as the regression fits of the same are shown by solid lines. The slopes of the graphical plot of log Fq(s) vs log (S)for different values of q (q=±5, 0) give the values of the generalised Hurst exponent $H_{q=+5}$= 0.84426, $H_{q=0}$= 0.91728 and $H_{q=-5}$= 0.95430 for q=+5, q=0 and q=-5 respectively. Mismatching of the values for generalised Hurst exponent for different values of q (q=±5, 0) as mentioned above confers that the soil radon time series is characterised with multiscaling properties. However in case of monofractal data or white noise these Hq values for different values of q (q=±5, 0) will be identical (i.e. $H_{q=+5}$= $H_{q=0}$= $H_{q=-5}$. Figure 6 shows the variations of the generalised Hurst exponent H_q for different values of q (q=±1 to ±5 and q= 0) (marked in blue symbol). It has been found that the value of H_q varies between a maxima 0.955 (for q= -5) and a minima 0.804 (for q= +5). The values of H_q seems to be higher for q < 0 in comparison to the values of H_q for q> 0. A similar feature was also observed by Kantelhardt et al. (2002) during the analysis of a non stationary time series data. This typical feature of H_q invokes that the soil radon time series content multifractal characteristics. Figure 6 also reveals that since the value of H_q always lies within $0.5<H_q<1$, the soil radon time series is characterized with persistent behavior. It is notable that if the value of H_q lies within $0<H_q<0.5$ the time series will show anti-persistence behaviour. Moreover, Figure 6 shows the variations of the generalized Hurst exponent for the shuffled time series (marked in red symbol) and that the values of $H_{q,shuf}$ remains around 0.5 with a minor dependence on the values of q. As the value of $H_{q,shuf}$ = 0.5, one may confer that the multifractality present in the soil radon time series likely to be originated out of the source type (b) as mentioned earlier i.e. due to long range correlations. The nature of dependence of scaling exponent τ on the values of q is shown in Figure 7.

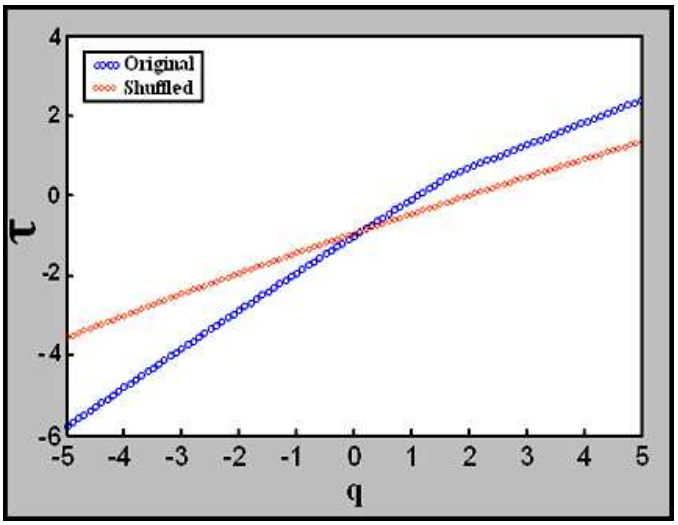

Figure 7. Variation of mass exponent (τ) with q for original time series (blue) and shuffled time series (red) for soil radon data.

For monofractal data set mass exponent shows linear dependence on the values of q. In the present case for soil radon data the mass exponent exhibits nonlinear characteristics with slope 0.60 for the region A (q= -5 to 1) and slope 0.36 for the region B (q =2 to 5). This implies that the nonlinearity is confined within the region C (q =1 to 2). In Figure 7 the variation of $\tau(q)$ with q for the original radon time series is represented by blue symbol while the same for the shuffled series is designated by red symbol. Since the variation of $\tau_{original}$ does not follow the same trend as the variation of $\tau_{shuffled,}$ one may conclude that the mutifractality present in the radon time series could be sourced from source type (b) as mentioned earlier i.e. due to long range correlations. Figure 8 shows the multifractal spectrum (graphical plot of D_q vs h_q, known as singularity spectrum) of the time series derived by MFDFA technique. The variation of D_q with h_q for the original radon time series is marked in blue symbol while the same for the shuffled time series is indicated in red symbol. Width of the spectrum for the original time series is $W_{original}$= 0.246 whereas for the shuffled one this value is $W_{shuffled}$ = 0.112. It is to be noted that width of the multifractal spectrum represents the degree of multifractality present in the time series. In the present case for the soil radon data $W_{original}>W_{shuffled}$ and therefore the shuffled series shows weaker multifractality in comparison to the original time series. This implies that apart from the source type (b) i.e. contribution from long range correlations, the multifractality of the soil radon time series was also sourced from the source type (a) i.e. broad probability density function. The maximum value of h_q(i.e. $h_{q,max}$) for which D_q attains its maximum value was estimated for the original radon time series. This value is estimated to be 0.9167. This relatively high value of $h_{q,max}$ (>>0) confers that the degree of correlation present in the said soil radon time series may be considered as an weaker coorelation. This suggests that the soil radon time series seems to be more irregular in pattern.

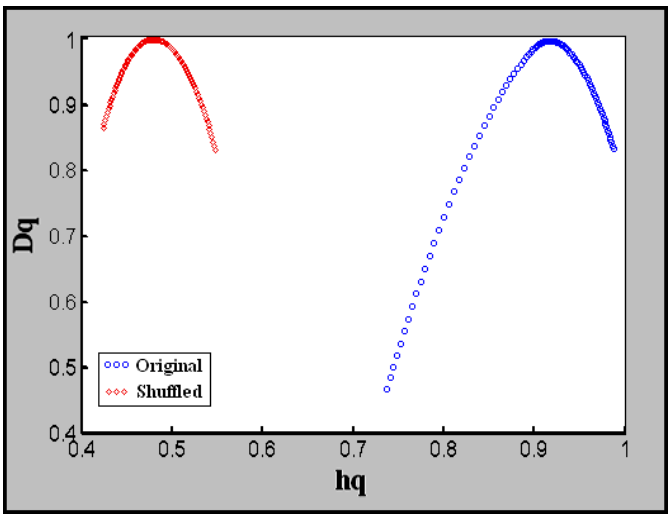

Figure 8. Multifractal spectrum of the original time series (blue) and shuffled time series (red) for soil radon data.

As mentioned earlier, out of four prominent fluctuations present in the entire time series as shown in Fig. 3 (panel A) there exist only two statistically valid large amplitude fluctuations (Fig. 4). Those two fluctuations were recorded during the periods December 20, 2012 and December 28-29, 2012 respectively. However, an average rainfall of 1.6 mm that continued for more than 20 hours was also recorded on December 28, 2012 (Fig. 3, pannel D). Consequently the anomalous decrease in the concentration of soil radon observed during December 28-29, 2012 likely to be associated with 1.6 mm rainfall on December 28, 2012. On the other hand, the soil radon anomaly observed during December 20, does not appear to be influenced either by rainfall or related meteorological criteria. It could be sourced from pre-seismic tectonic activities and may be well treated as a seismic induced anomaly. The said negative anomaly was well below M-2σ and also sustained for more than 10 hours on December 20, 2012. Now, in order to assign the probable seismic events that sourced the observed soil radon anomaly, we consider all the 51 earthquakes (magnitude > 4*M*) that occurred in India and its neighborhood during the two month time period November 1, 2012 to January 10, 2013. The regional occurrences of the listed earthquakes were within a radius of 1000 km from the Tattapani monitoring laboratory. Seismological data was collected from the India Meteorological Department (IMD) and the US Geological Survey (USGS) website reports (http://www.imd.gov.in/ section/seismo/dynamic & http://earthquake.usgs.gov/earthquakes) for the study period Nov 12 to Jan 2013.

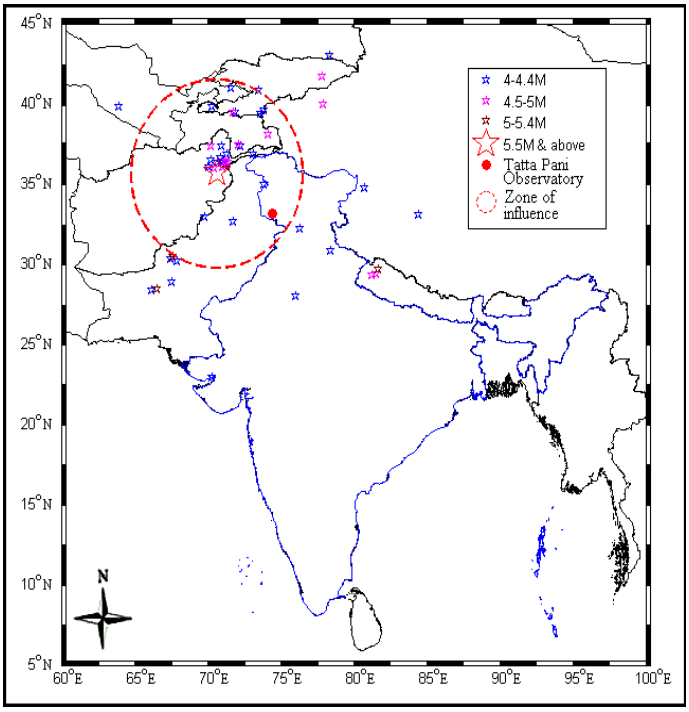

Figure 9. Seismological data of the earthquakes that occurred within a radius of 1000 km from the Tattapani observatory during the period of November 1, 2012 – January 10, 2013.

Magnitude wise epicenter within 1000 km of Tattapani for the study period area is shown in Figure 9. Tattapani lies within 500 km of the M 5.9 HinduKush earthquake epicenter as shown by the circle. The maximum radius of precursory zone (R_{max}) for each event was estimated using equation (12). We put forward the argument that an impending earthquake may generate anomalies in soil radon concentrations provided the distance between the monitoring site and the earthquake epicenter (D_E) is approximately close to or less than R_{max} i.e., (i) $D_E \sim R_{max}$ or (ii) $D_E \leq R_{max}$. A similar approach was also followed by Chaudhuri et al., 2011; Walia et al., 2013 to find out correlation between observed radon anomaly and subsequent seismic events. Out of all the 51 listed earthquakes (shown in Fig 9) only one instance (red star symbol), the Hindukush region (35.711^0N; 70.599^0E) earthquake of magnitude 5.9M that occurred on December 29, 2012 satisfies the distance rule (ii) D_E (=443 km) $<R_{max}$(=679 km). Consequently the soil radon anomaly observed during the period December 20, 2012 may be considered as a genuine precursor for the 5.9M Hindukush region earthquake that occurred on December 29, 2012. The mentioned negative anomaly was observed 9 days prior to the Hindukush region earthquake.

6. Conclusion

The technique of MFDFA helps to identify four prominent fluctuations (> mean+2σ and also < mean-2σ) in the entire two months radon time series data recorded at Tattapani laboratory. Out of four prominent fluctuations observed in the soil radon time series only two fluctuations were identified as statistically valid large amplitude fluctuations using the RMS analysis. Any cross-correlation between the temporal variation of concentration profile of soil radon, soil temperature as well as soil pressure was not found. However, the anomalous decrease in the concentration of soil radon (large amplitude fluctuation) observed during December 28-29, 2012 is likely to be associated with 1.6 mm rainfall on December 28, 2012 and was not sourced from any seismic activity. Moreover the distance rule incorporating the estimation of the epicentral distance and maximum radius of precursory zone suggests that the soil radon anomaly observed during the period December 20, 2012 (the remaining large magnitude fluctuation) may be considered as a genuine precursor for the 5.9M Hindukush region earthquake that occurred on December 29, 2012.

The method of MFDFA also assists to figure out the underlying dynamics of radon emanation process from soil gas. Mismatching of the estimated values for generalised Hurst exponent for different values of q (q = ±5, 0) confers that the soil radon time series was characterised with multiscaling properties. Moreover since the estimated values of H_q always lies within $0.5<H_q<1$, one may confer that the soil radon time series is characterized with persistent behavior. The estimated value 0.5 of the generalized Hurst exponent for the shuffled time series ($H_{q,shuf}$) suggests that the multifractality present in the soil radon time

series likely to be originated out of the source contribution from long range correlations. For the radon time series data the estimated width of the multifractal spectrum for the original time series ($W_{original}$) seems to be greater than the width of the multifractal spectrum for the shuffled time series ($W_{shuffled}$). This implies that apart from the source of multifractality from contribution from long range correlations, the multifractality of the soil radon time series was also sourced from the broad probability density function. Relatively high value of the estimated Hölder exponent $h_{q,max}$ (>>0) for the soil radon time series data implies that the soil radon time series seems to be more irregular in pattern. The method of MFDFA seems to be potential tool to explore the underlying physics inherent in the time series data related with soil radon anomaly for the study of earthquake precursors.

Acknowledgments

The authors gratefully acknowledge the financial support of the Ministry of Earth Sciences (MoES), New-Delhi, under Project No. MoES/P.O.(Seismo)/NPEP(14)/2009 dated 18.03.2010 under which this work was carried out. The authors also greatly acknowledge institutional support provided by the Department of Atomic Energy, Variable Energy Cyclotron Centre, Kolkata, for this research. Special thanks are also expressed to Shri. Sumit Khajuria and others colleagues from Tattapani Geochemical Monitoring Laboratory, J & K for their assistance.

References

Abumuard, K. M., and M. Al-Tamimi (2001). Emanation power of radon and its concentration in soil and rocks, *Radiation Measurements,* 34, 423–426.

Ashkenazy Y, D. K. Baker, H. Gildor, and S. Havlin (2003a). Nonlinearity and multifractality of climate change in the past 420,000 years, *Geophysical Research Letters,* 30, 2146-2149.

Ashkenazy, Y., S. Havlin, P. C. Ivanov, C. K. Peng, V. Schulte-Frohlinde, and H. E. Stanley (2003b). Magnitude and sign scaling in power law correlated time series, *Physica A,* 323, 19-41.

Ball, T. K. (1994). Temporal variation in soil gas according to soil types, In: Radon Investigations in Czech Republic, Barnet I and Neznal M, Eds Praha: Geological Survey and Radon Corp, 5, 127–128.

Barabási, A. L., and T. Vicsek (1991). Multifractality of self-affine fractals, *Physical Review A,* 44, 2730-2733.

Barnet, Y., A. Kies, L. Skalsk´y, and J. Procházka (1997). Radon variations and Earth tides in unventilated underground spaces, *Bulletin of the Czech Geological Survey,* 72, 105–114.

Bhat, G. M., R. Ghara, and S. Kaul (2009). Potential for oil and gas in the Proterozoic carbonates Sirban Limestones of Jammu, Northern India, *Geological Society of London* (Special Publications) 476, 371-396.

Chaudhuri , H., D. Ghose, R. K. Bhandari, P. Sen, and B. Sinha (2012). A geochemical approach to earthquake reconnaissance at the Baratang mud volcano, Andaman and Nicobar Islands, *Journal of Asian Earth Science,* 46, 52–60, 2012, doi:10.1016/j.jseaes.2011.10.007.

Chaudhuri, H, N. K. Das, R. K. Bhandari, D. Ghose, P. Sen, and B. Sinha (2010b). Radon activity measurements around Bakreswar Thermal Springs, *Radiation Measurements,* 45, 143-146, doi: 10.1016/j.radmeas.2009.11.039.

Chaudhuri, H., C. Barman, A. N. S. Iyengar, D. Ghose, P. Sen, and B. Sinha (2013a). Network of seismo-geochemical monitoring observatories for earthquake prediction research in India, *Acta Geophysica,* 61, 1000-1025, doi: 10.2478/s11600-013-0134-0.

Chaudhuri, H., C. Barman, A. N. S. Iyengar, D. Ghose, P. Sen, and B. Sinha (2013b). Long range correlation in earthquake precursory signals, *The European Physical Journal* (Special Topics), 222, 827-838, doi: 10.1140/epjst/e2013-01886-y.

Chaudhuri, H., D. Ghose, R. K. Bhandari, P. Sen, and B. Sinha (2010a). The Enigma of Helium, *Acta Geodaetica et Geophysica Hungarica,* 45, 452–470, doi:10.1556/AGeod.45.2010. 4.5, 2010.

Chaudhuri, H., W. Bari, N. Iqbal, R. K. Bhandari, D. Ghose, P. Sen, B. Sinha (2011). Long range gas- geochemical anomalies of a remote earthquake recorded simultaneously at distant monitoring stations in India, *Geochemical Journal,* 45, 137-156.

Chen Z, P. C. Ivanov, K. Hu, and H. E. Stanley (2002). Effect of nonstationarities on detrended fluctuation analysis, *Physical Review E,* 65, 041107-41122.

Cicerone, R. D., J. E. Ebel and J. Britton (2009). A systematic compilation of earthquake precursors, *Tectonophysics,* 476, 371–396.

Das, N. K., H. Chaudhuri, D. Ghose, R. K. Bhandari, P. Sen, and B. Sinha (2006b). Nonlinear analysis of radon time series related to earthquake, Modelling Critical and Catastrophic Phenomena in Geoscience, Lecture Notes in Physics, 705, 481-490, Springer-Verlag. Berlin Heidelberg, ISBN: 978-3-540-35373-7.

Das, N. K., H. Chaudhuri, R. K. Bhandari, D. Ghose, P. Sen and B. Sinha (2006a). Continuous monitoring of 222Rn and its progeny at a remote station for seismic hazard surveillance, *Radiation Measurements,* 41, 634-637, doi:10.1016/j.radmeas. 2006.03.003.

Davis, A., A. Marshak, W. Wiscombe, and R. Cahalan (1994). Multifractal characterizations of nonstationarity and intermittency in geophysical fields: Observed, retrieved, or simulated, *Journal of Geophysical Research,* 99 D4, 8055-8072.

Deidda, R. (2000). Rainfall downscaling in a space-time multifractal framework, *Water Resources Research,* 36, 1179-1794.

Dutta, S. (2010a). Multifractal detrended fluctuation analysis of SENSEX fluctuation in the Indian stock market, *Canadian Journal of Physics,* 88, 545-551.

Dutta, S. (2010b). Multifractal properties of ECG patterns of patients suffering from congestive heart failure, *Journal of Statistical Mechanics: Theory and Experiment,* 12, 12021-12035.

Feder, J. (1988). Fractals, Plenum Press, New York.

Fleischer, R. L. (1981). Dislocation model for radon response to distant earthquakes, *Geophysical Research Letters,* 8, 477-480.s

Ghosh, D., A. Deb, and R. Sengupta (2009). Anomalous radon emission as precursor of earthquake, *Journal of Applied Geophysics,* 69, 67-81.

Ghosh, D., A. Deb, S. Dutta, R. Sengupta, and S. Samanta (2012). Multifractality of radon concentration fluctuation in earthquake related signal, *Fractals,* 20, 33-39.

Gokam, S. G., C. K. Rao, and G. Gupta (2002). Crustal structure in the Siwalik Himalayas using magnetotelluric studies. *Earth, Planets and Space,* 54, 19–30.

Hartmann, J., and J. K. Levy (2005). Hydrogeological and gasgeochemical earthquake precursors: a review for application, *Natural Hazards,* 34, 279–304.

Hassan, M. U. M., and M. S. Baig (2006). Paleogene biostratigraphy of Tattapani, Kotli Azad Kashmir, northwest sub-Himalayas, Pakistan, *Journal of Himalayan Earth Sciences,* 39, 39–48.

Hauksson, E., and J. G. Goddard (1981). Radon earthquake precursor studies in Iceland, *Journal of Geophysical Research,* 86, 7037–7054.

Holub, R. F. and B. T. Brady (1981). The effect of stress on radon emanation from rock, *Journal of Geophysical Research,* 86B3, 1776-1784.

Hu, J., J. Gao, and X. Wang (2009). Multifractal analysis of sunspot time series: the effects of the 11-year cycle and Fourier truncation, *Journal of Statistical Mechanics: Theory and Experiment,* 02, P02066.

Hu, K., P. C. Ivanov, Z. Chen, P. Carpena, and H. E. Stanley (2001). Effect of trends on detrended fluctuation analysis, *Physical Review E,* 64, 01114-01133.

Igarashi, G., and H. Wakita (1990). Groundwater radon anomalies associated with earthquakes, *Tectonophysics*, 180, 237–254.

Ihlen E. A. F. (2012). Introduction to multifractal detrended fluctuation analysis in Matlab, *Frontiers in Physiology,* 3, 1-18.

India Meteorological Department IMD website reports http://www.imd.gov.in /section /seismo/ dynamic/welcome.htm

Ivanov, P. C., L. A. N. Amaral, A. L. Goldberger, S. Havlin, M. G. Rosenblum, Z. R. Struzik, and J. W. Kantelhardt, S. A. Zschiegner, E. K. Bunde, and A. Bunde (2002). Multifractal detrended Fluctuation Analysis of Nonstationary Time Series, *Physica A,* 316, 87-114.

Kantelhardt, J. W., R. Berkovits, S. Havlin, and A. Bunde (1999). Are the phases in the Anderson model long-range correlated?, *Physica A,* 266, 461-464.

Kantelhardt, J. W., E. Koscielny-Bunde, H. H. A. Rego, S. Havlin and A. Bunde (2001). Detecting long-range correlations with detrended fluctuation analysis, *Physica A,* 295, 441-454.

King, C. Y. (1980). Episodic radon changes in in subsurface soil gas along active faults and possible relation to earthquakes, *Journal of Geophysical Research,* 85, 3065-3078.

Kumar, A., V. Walia, S. Singh, B. S. Bajwa, S. Mahajan, S. Dhar, and T. F. Yang (2012). Earthquake precursory studies at Amritsar Punjab, India using radon measurement techniques, *International Journal of Physical Sciences,* 7, 5669-5677.

Liu, Y., P. Gopikrishnan, P. Cizeau, M. Meyer, C. K. Peng, and H. E. Stanley (1999). Statistical properties of the volatility of price fluctuations, *Physical Review E,* 60, 1390-1400.

Movahed, M. S., G. R. Jafari, F. Ghasemi, S. Rahvar, and M. R. R. Tabar (2006). Multifractal detrended fluctuation analysis of sunspot time series, *Journal of Statistical Mechanics: Theory and Experiment,* 02, P02003.

Muzy, J. F., E. Bacry, and A. Arneodo (1991). Wavelets and multifractal formalism for singular signals: Application to turbulence data, *Physical Review Letters,* 67, 3515-3518.

Nazaroff, W. W., and A. V. Nero Eds (1988). Soil as a source of indoor radon: generation, migration and entry: Radon and its decay products in indoor air, Wiley-Inter-science publication, 57–112.

Peng, C. K., S. V. Buldyrev, S. Havlin, M. Simons, H. E. Stanley, and A. L. Goldberger (1994). Mosaic organization of DNA nucleotides, *Physical Review E,* 49, 1685-1689.

Planinic, J., V. Radolic, and B. Vukovik (2004). Radon as an earthquake precursor, *Nuclear Instruments and Methods A*, 530, 568–574.

Prasad, Y., G. Prasad, M. S. Negi, V. M. Choubey, and R. C. Ramola (2006). Variation of Radon levels in spring water with meteorological parameters and seismic events in Garhwal Himalaya, *Environmental Geochemistry,* 9, 76-79.

Rai, R.P., A. Singh, R. S. Acharya, and A. K. Singh (1996). Role of geophysics in deciphering geothermal channel in Tattapani area, Rajouri District, Jammu and Kashmir, *Journal of Geological Society of India,* 45, 234-248.

Ramola, R. C., Y. Prasad, G. Prasad, S. Kumar, and V. M. Choubey (2008). Soil-gas radon as seismotectonic indicator in Garhwal Himalaya, *Journal of Applied Radiation and Isotopes,* 66, 1523-1530.

Schynoll, J., and S. D. Chatterjee (1958). On the therapeutic effects of the thermal waters of Bakreswar, *Science and Culture,* 23, 591-594.

Shankar, R. (1991). Distribution of thermal springs in North-Western India J&K, Himachal Pradesh, Parts of Uttar Pradesh and Haryana, Geothermal Atlas of India, *Journal of Geological Society of India,* 19, 10-13.

Shimizu, Y., S. Thurner, and K. Ehrenberger (2002). Multifractal spectra as a Measure of complexity in human posture, *Fractals,* 10, 103-116.

Siva, S. N. (2011). Origin of chert breccias at the unconformity between Precambrian Sirban Limestone and Palcogenic Subathu Formation: evidence from Kalakot area, J&K Himalaya, *Current Science,* 100, 1875-1880.

Stanley, H. E. (1999). Multifractality in human heartbeat dynamics, *Nature* 399, 461-465.

Talwani, P. (1979). An empirical earthquake prediction model, *Physics of the Earth and Planetary Interiors,* 18, 288-302.

Telesca, L., and V. Lapenna (2006). Measuring multifractality in seismic sequences, *Tectonophysics,* 423, 115-123.

Telesca, L., M. Balasco, G. Colangelo, V. Lapenna, and M. Macchiato (2004). Investigating the multifractal properties of geoelectrical signals measured in southern Italy, *Physics and Chemistry of the Earth,* 29, 295–303.

Telesca, L.,V. Lapenna and M. Macchiato (2005). Multifractal fluctuations in earthquake-related geoelectrical signals, *New Journal of Physics,* 7, 214.

Tessier, Y., S. Lovejoy, and D. Schertzer (1993). Universal Multifractals: Theory and Observation for Rain and Clouds, *Journal of Applied Meteorology,* 32, 223-250.

Toutain, J. P., and J. C. Baubron, (1999). Gas geochemistry and seismotectonics: A review, *Tectonophyics,* 304, 1-27.

USGS website report, Available online at http://earthquake.usgs.gov/earthquakes/eqarchives/epic/epic_circ.php

Vandewalle, N., M. Ausloos, M. Houssa, P. W. Mertens, and M. M. Heyns (1999). Non-Gaussian behavior and anticorrelations in ultrathin gate oxides after soft breakdown, *Applied Physics Letters,* 74, 1579- 1582.

Virk, H. S., and B. Singh (1993). Radon anomalies in soil-gas and groundwater as earthquake precursor phenomena, *Tectonophysics,* 227, 215-224.

Wadia, D. N. (1928). The geology of Poonch State Kashmir and adjacent portions of the Punjab, *Memoirs Geological Survey of India,* 51, 185–370.

Wakita, H. (1996). Geochemical challenges to earthquake prediction, *Proceedings of the National Academy of Sciences* USA, 93, 3781-3786.

Walia, V., B. S. Bajwa, H. S. Virk, and N. Sharma (2003). Relationships between seismic parameters and amplitudes of radon anomalies in N-W Himalaya, India, *Radiation Measurements,* 36, 393-396.

Walia, V., T. C. Su, C. C. Fu, and T. F. Yang (2005a). Spatial variation of radon and helium concentration in soil- gas across Shan Chiaon fault, Northern Taiwan*, Radiation Measurements,* 40, 513-516.

Walia, V., H. S. Virk, T. F. Yang, S. Mahajan, M. Walia, and B. S. Bajwa (2005b). Earthquake Prediction Studies usion Radon as a Precursor in N-W Himalayas, India: A case study, *Terrestrial Atmospheric and Oceanic Sciences,* 16, 775-804.

Walia, V., S. J. Lin, W. L. Hong, C. C. Fu, T. F. Yang, K. L. Wen, and C. H. Chen (2009). Continuous temporal soil-gas composition variation for earthquake precursory studies along Hsincheng and Hsinhua faults in Taiwan, *Radiation Measurements,* 44, 934-939.

Walia, V., T. F. Yang, S. J. Lin, A. Kumar, C. C. Fu, J. M. Chiu, H. H. Chang, K. L. Wen and C. H. Chen (2013). Temporal variation of soil gas compositions for earthquake surveillance in Taiwan, *Radiation Measurements,* 50, 154-159.

Weinlich, F. H., E. Faber, A. Boušková, J. Horálek, M. Teschner, and J. Poggenburg (2006). Seismically induced variations in MariánskéLázně fault gas composition in the NW Bohemian swarm quake region, Czech Republic- A continuous gas monitoring, *Tectonophys*ics, 421, 89-110.